PCCP

Chirped Pulse Fourier-Transform Microwave Spectroscopy of Alcohol and Water Tetramers

Journal:	*Physical Chemistry Chemical Physics*
Manuscript ID	CP-ART-10-2022-005022.R1
Article Type:	Paper
Date Submitted by the Author:	20-Dec-2022
Complete List of Authors:	Dutton, Sarah; California Institute of Technology, Chemistry Mastin, Evan; California Institute of Technology Blake, Geoffrey; California Institute of Technology, Division of Geology and Planetary Science; California Institute of Technology, Division of Chemistry and Chemical Engineering

PCCP

ARTICLE TYPE

Cite this: DOI: 00.0000/xxxxxxxxxx

Chirped Pulse Fourier-Transform Microwave Spectroscopy of Alcohol and Water Tetramers

S. E. Dutton,* E. M. Mastin, * and G. A. Blake*

Received Date
Accepted Date

DOI: 00.0000/xxxxxxxxxx

In an effort to build towards quantitative models of alcohol:water microaggregation in liquid mixtures, the present works characterizes the energy landscape and structures of pure ethanol and mixed ethanol:water tetramers using Chirped Pulse Fourier-transform Microwave spectroscopy. Many conformers of each type of tetramer are available, and those with sufficiently strong dipole moments are experimentally examined. This analysis considers, but does not explicitly fit, the splitting of rotational states due to internal rotation of the methyl groups present, as well as utilizes isotopic substitution experiments to verify the conformer variations observed. Implications of the listed results include a suggestion of the stability of micro-aggregated structures as opposed to homogeneously mixed clusters, informing future work on characterization of larger clusters and any potential modeling of the hydrogen bond network at play.

1 Introduction

From protein solvation to aqueous geochemistry, a vast array of modeling relies on accurately constraining the interactions of few water molecules at a time [1–5]. This few-atom computational problem is non-trivial however, as the network of hydrogen bonding defining the intermolecular potential energy surface of water is complex, and traditionally difficult to study.

Recent advances in coherent, broadband microwave and terahertz generation and spectroscopic technologies have opened the door for more detailed studies of water on micro-scale [6,7]. As these questions begin to be answered, more arise as to how this hydrogen bond network of water aggregation is disrupted by other small molecule hydrogen bond donors and acceptors, such as low molecular weight alcohols. Understanding alcohol:water mixing at a few-molecule scale carries weight for understanding the bulk properties, and the anomalous negative entropy of mixing characteristic of these substances [8–10], for understanding solvation effects for reactions conducted in alcohol:water solvents [11,12], and even for the physicochemical and antiviral/antibacterial properties of hand sanitizer [13,14], particularly relevant during this period of heightened demand.

To begin building an understanding of the local environment of water:alcohol mixing, a precise potential energy surface of few molecule interactions is required. The best tool to start mapping this small cluster energy landscape is Chirped Pulse Fourier-transform MicroWave spectroscopy, or CPFTMW [15–18]. By yielding experimentally determined rotational constants, this technique provides an atomically-accurate geometry of small molecule clusters of interest, showing the bonding pattern and determining which out of multiple minima on the potential energy surface for a potential cluster are physically observed. In addition, the high spectral resolution of this technique allows for fitting of split rotational states due to internal rotation or tunneling, not just the vibrationally averaged minimum geometry.

In the present work, pure ethanol and water:ethanol tetramers are targeted, in an effort to understand the asymmetric geometry that allows for a net dipole in these clusters, and to elucidate the patterns of micro-aggregation of water and ethanol vs. the homogeneous distribution of these species throughout the tetramer. Multiple conformers of most tetramers are observed, and confirmed through isotopic substitution. In addition, splitting and line center displacements in the rotational spectra due to internal rotation of the methyl groups in ethanol are investigated [19,20], and estimated computationally.

2 Experimental

Following the work of Mejía et al [21], the lowest energy structures of the pure ethanol and mixed water:ethanol tetramers were optimized with Gaussian 16 [22]. Local minima were identified, and anharmonic corrections to rotational constants were retrieved using the DFT method at the B3LYP level of theory and the 6311g++G(d,p) basis set. Previous work had shown that this level of theory and basis set were sufficient for calculating approximate rotational constants [16,21,23]. Relative energies of all the calculated conformers of ethanol:water tetramers are shown in the Supplementary Information, where a trend of increasing energy with increased water content in the tetramers is evident.

*Division of Chemistry and Chemical Engineering, California Institute of Technology, 1200 E California Blvd., Pasadena, CA 91125, USA. E-mail: gab@gps.caltech.edu

† Electronic Supplementary Information (ESI) available. See DOI: 10.1039/cXCP00000x/

As expected from the cyclic water tetramer, all cluster conformers are based on a motif where the ethanol and water monomers act as both a hydrogen bond donor and acceptor. To further refine the cluster geometries, experimental spectra were collected using the Blake Group high throughput CPFTMW apparatus described previously[24]. Clusters were formed by bubbling argon through solely ethanol or separate flasks of ethanol and water at a backing pressure of 1.5 atm, with the water flask heated to approximately 60 C to form clusters with higher water content. The gas stream was expanded continuously through a 10 cm $\times$ 25 μm slit nozzle into the vacuum chamber, and the background pressure was kept below $4 * 10^{-4}$ torr during the continuous expansion. After each excitation pulse, free induction decays (FIDs) of 18 microseconds were collected, and 200 million were averaged together at a time for each local oscillator (LO) setting. This corresponded to a wall clock experiment time of just over 2 hours for each LO setting. The signal-to-noise ratio for the monomer lines observed was on the order of 3000:1, and for the tetramer lines detected, it was on the order of 10:1. A sample of the experimental spectra collected, with assigned lines, is shown in Figure 1.

For the pure ethanol tetramer, there were three lowest energy conformers identified in previous work, denoted 2g-2g+, 2g-g+t, and 2tg+g-. Depictions of these conformers and their relative energies are shown in Figure 2. Of these conformers, only the 2tg+g- conformer had a dipole moment of sufficient strength, that is, above 0.4 debye, to be seen via chirped pulse rotational spectra with the available microwave peak power. This conformer was the highest in energy out of the computed minima structures, however the difference in energy between the conformers, around 0.1 kcal/mol, was small enough that we would expect to see all conformers forming in the supersonic expansion. Previous work studying the dimerization of ethanol has shown a similar trend in the supersonic expansion experimental signatures of conformers with similar energy, in which all of these low-energy conformers were identified[25]. This work therefore supports the conclusion that all low-lying conformers with sufficiently large dipole moments should be observable in the expansion.

Of the 30 conformers of $(H_2O)(CH_3CH_2OH)_3$ clusters reported previously, the lowest nine in energy were minimized in Gaussian. Of those, many are highly symmetric, leading to a low dipole moment and therefore experimental challenges to observe the structures in rotational spectra. Altogether, two of these eight most stable conformers have net dipole moments about 0.3 debye, and were identified in experimental spectra. These structures are denoted wttt and wg1g2t, according to the relative conformation of the ethanol subunits; wttt has all trans ethanol, wg1g2t has two gauche ethanol molecules, on opposite sides of the plane of hydrogen bonding, and one trans molecule. Figure 2 shows that while these two conformers are not the lowest in energy of all the conformers with one water calculated, they are the only conformers with a large enough dipole moments. Thus, while other conformers of $(H_2O)(CH_3CH_2OH)_3$ are lower in energy, and likely formed during the expansion of water and ethanol, they are not detectable in the spectra collected.

Similarly, two conformers of $(H_2O)_2(CH_3CH_2OH)_2$ clusters were observed in the spectra. Previous computational work has not included a full survey of these clusters, so the cyclic forms of these clusters were optimized by building on the work of Mejía et al. and substituting an additional water molecule into the cyclic mixed tetramer structures. Every variation of gauche and trans geometry for the ethanol molecules was combined with every variation of relative position around the ring of hydrogen bonding. It was observed that these structures were all very close in energy, spanning under 0.1 kcal/mol in total. In addition, of these structures, few had dipole moments sufficient to give an observed signal experimentally, similarly to the one water clusters. The two conformers with sufficiently high dipoles were those denoted wg1tw and wttw, one with both ethanol groups in trans conformations, and another with one trans ethanol and one gauche.

Finally, the $(H_2O)_3(CH_3CH_2OH)$ cluster was studied; two conformations of the structure with circular hydrogen bonding are present, corresponding to the two conformers of ethanol. These two different conformers of the three-water cluster are again close in energy, and each has a low net dipole. By increasing backing pressure of the Argon carrier gas to 2 atm, and increasing temperature of the water sample to approximately 60 C, production of these tetramers was optimized, and both conformers were identified in the spectra. These are referred to as twww and gwww, referring to the trans configuration of the ethanol sub-unit vs. the gauche, as can be seen in Figure 3.

3 Results

The implementation of CPFTMW used to target ethanol and ethanol:water clusters described above yielded spectra spanning 10 to 18 GHz, with signal to noise ratios on the lines of interest of $\geq$10:1. From these spectra, a, b and c type transitions were fit for all observed conformers, with a-type transitions most abundantly observed, consistent with this being the strongest dipole moment component of the tetramers. These transitions correspond to J values ranging from around 10 to 20 for higher ethanol content clusters, and 5 to 10 for higher water content clusters.

To confirm individual line assignments, dual resonance experiments were conducted on the strongest lines observed for each conformer. This allowed for definitive assessment of how the rotational states observed related to each other, supporting the correct assignment of quantum states. With these appropriately assigned lines, experimental rotational constants were retrieved using the program SPFIT[26]. Comparisons of calculated rotational constants and anharmonic correction terms to experimentally determined values are shown in Table 1 for the pure ethanol tetramer conformers, Table 2 for the $(H_2O)(CH_3CH_2OH)_3$ conformers, Table 3 for the $(H_2O)_2(CH_3CH_2OH)_2$ conformers, and Table 4 for the $(H_2O)_3(CH_3CH_2OH)$ conformers. Distortion constants were fit with SPFIT, but omitted from final fits with a low number of lines available in the spectra. The robusticity of the fits for A, B, and C rotational constants is such that geometry of the clusters can be predicted to high precision, and are in good agreement with the calculated rotational constants.

Experimental line strengths indicate a rotational temperature of $\sim$10 K when compared with simulated spectra. Populations among cluster types are less straightforward to estimate, given weak lines and highly dense spectra observed, but from compar-

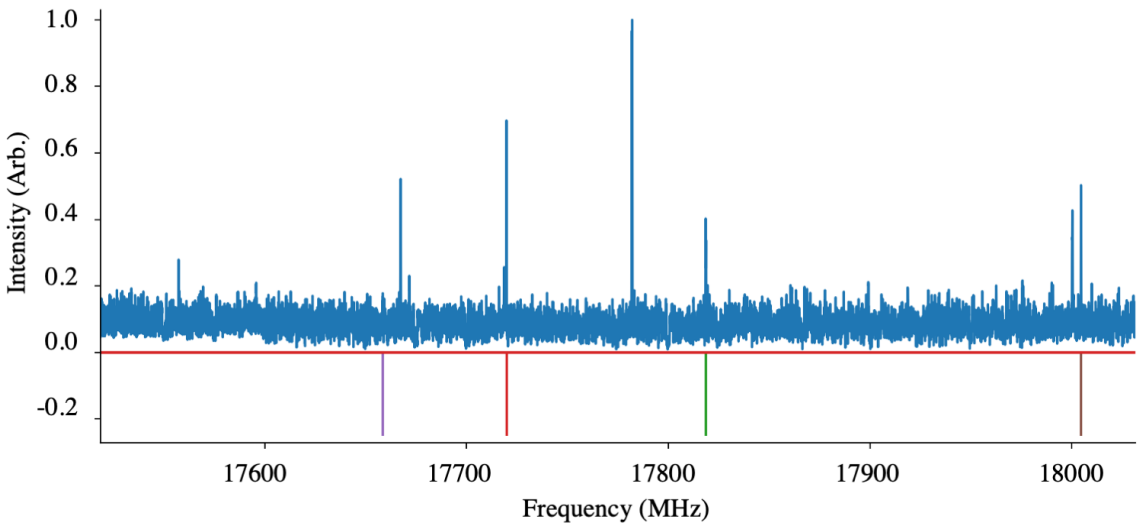

Fig. 1 Section of experimental spectrum with lines fit for various EtOH-water tetramer species. Pictured are lines fit to the $(H_2O)_2(C_2H_5OH)_2$ wg1tw (green)/wttw (red) and $(H_2O)(C_2H_5OH)_3$ wg1g2t (purple)/wttt (brown) tetramers

.

ing line strengths in fairly narrow spectral windows and transitions with similar predicted intensities, we see that relative ratios of conformers vary from 1:1 to 5:1. When these ratios are scaled with respect to the predicted energy differences between the conformers, there is no clear trend that could be used to estimate a vibrational temperature that could explain the relatives populations among cluster types. This may be due to the fact that many conformers of each tetramer are undetectable with the current instrument, given their low dipole moment projections. What does seem to follow is that when there are fewer available conformers in a certain cluster type, i.e. only two available conformers (twww and gwww) for the three water tetramer, the relative populations (when corrected for the different predicted dipole moments) are noticeably different, close to a 5:1 ratio that favors the lower energy cluster. For the cases where more cluster geometries are close in energy, such as one water and two water tetramers, the relative populations are more even, indicating a more stochastic distribution between the accessible conformers. Taken together, the results do imply a somewhat higher vibrational (or conformer) temperature than rotational excitation temperature within a given cluster. This is consistent with previous pinhole expansion experiments, but the difference is perhaps smaller (as demonstrated by the three water cluster populations), and likely due to the more extensive soft collisional environment afforded by a slit nozzle.

To additionally confirm conformer assignment, isotopically enriched samples were used to experimentally compare hydrogen positions within the observed tetramer conformers. From these deuterated sample experiments, isotopologues of each conformer were observed in the spectra, confirming assignment of every conformer reported herein. Figure 4 shows the substituted geometry compared to the assigned conformer hydrogen position for two conformers as an example. In addition, hydrogen exchange during sample preparation or data acquisition with D_2O led to the formation of HDO as well, thus allowing for tetramer clusters to form with single isotopic substitution in the water subunits. These singly substituted species for each conformer were fit, and Kraitchman analysis performed to calculate H position for a donated H from a water molecule[27]. Singly deuterated ethanol was also formed during hydrogen exchanged, but these isotopologues were not fit due to low abundance. For further details on experimentally fitting these isotopologues, see the Supplementary Information. The results of the perdeutero fits provide additional data as to the the accuracy of modeled rotational constants with fit rotational constants, in addition to qualitatively confirming the correct conformer assignment of the observed tetramers. To further confirm these conformer assignments and geometries, the results from the singly deuterated isotologues allow us to quantitatively calculate the hydrogen position via the Kraitchman equations.

When fitting some transitions for the tetramer species observed, higher error than experimental precision was observed, especially for transitions from high J states. This higher error can be explained by the internal rotation of the methyl groups present in these clusters, which splits the rotational transitions observed. The magnitude of this splitting is directly proportional to the height of the barrier to methyl group rotation. For the ethanol monomer this barrier is $\sim$1185 cm^{-1} for the trans conformer $\sim$1250 cm^{-1} for the gauche conformer[28]. This high of a barrier leads to a low magnitude of splitting of the rotational states, up to a few tens of kilohertz.

To model the splitting of rotational states in mixed ethanol and water tetramers due to internal rotation, the program XIAM[29] was used. This program works well to model splitting from up to two internal rotors, thus tetramers with additional rotors were simplified by assuming that rotors with similar local environments and similar geometry within a conformer could be approximated to be the same type of rotor. The output of XIAM is therefore an approximation, as the geometry inputs do not reflect all the internal rotation possible in some of the tetramers. This is sufficient however, as we are more interested in the magnitude of the

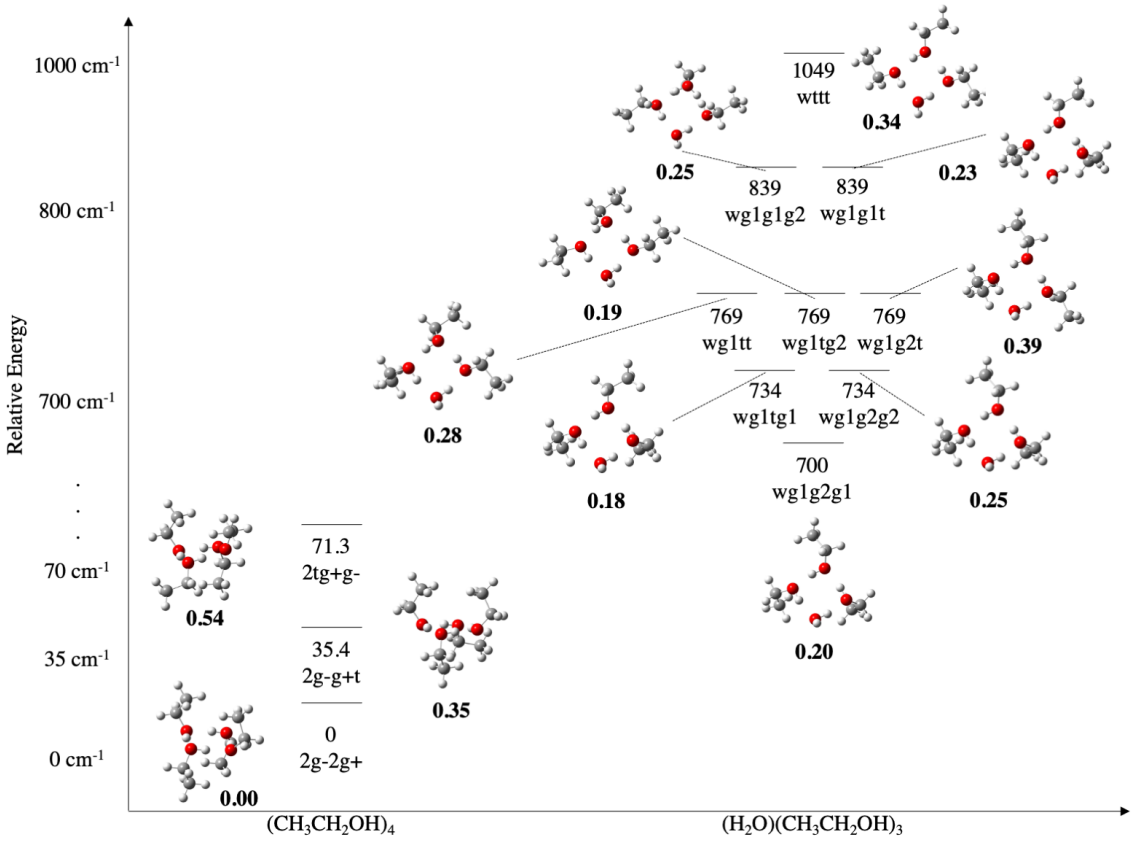

Fig. 2 Relative energies of the lowest three conformers of the pure ethanol tetramer and lowest nine conformers of $(H_2O)(CH_3CH_2OH)_3$. Dipole moments (in debyes) listed below the figure of each conformer. Jump in energy corresponds to difference in tetramerization energies of $(CH_3CH_2OH)_4$ and $(H_2O)(CH_3CH_2OH)_3$ from the literature[21].

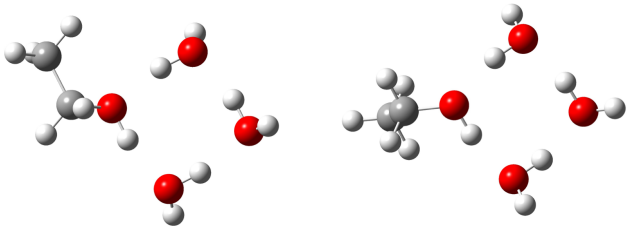

Fig. 3 Comparison of gauche and trans geometry between $(H_2O)_3(CH_3CH_2OH)$ conformers.

splitting of rotational states than the absolute line positions.

The magnitude of this splitting of rotational states due to internal rotation was thus determined to be on the order of 10 kHz, which supports the increased error we see in line assignment. This low-level splitting is too small for us to resolve with our instrumentation however; higher resolution could be achieved with the use of a large cavity, coaxial Flygare instrument.

The results of these isotopologue fits show good agreement between calculated rotational constants and fitted rotational constants, thus implying that the modeled geometries are good approximations of the true vibrationally averaged structures. From the conformers observed in experimental data, a trend appears in calculated average O-O bond distance. This distance increases for mixed tetramers, but as progressively more water is incorporated into the ethanol tetramers, average O-O bond distance decreases. For pure ethanol tetramers, this distance is on average 2.71 to 2.72 Angstroms, depending on the conformer. For $(H_2O)(CH_3CH_2OH)_3$ tetramers, this average distance is around to 2.75 Angstroms, then is essentially the same at 2.74 for $(H_2O)_3(CH_3CH_2OH)$ clusters. This same pattern is observed for trimers; O-O distance is increased in mixed trimers. For full details, see Supplementary Information.

This trend in O-O distance speaks to the strength of hydrogen bonds in these pure and mixed clusters. The increase in distance implies a weakening of interaction strength between water and ethanol, then a successive increase in hydrogen bonding strength as more water is substituted into the clusters. This may be explained by the higher cooperativity available to water, given the multiple hydrogen bond acceptor and donor sites on water. This potential for higher cooperativity allows for water to bond in more compact, three dimensional geometric patterns as cluster size increases, as seen in previous work[30–35]. This cooperativity is limited in pure ethanol clusters, and in addition, the steric hindrance of the carbon chain further weakens the hydrogen bonding interaction in mixed water:ethanol tetramers. Of note, then, is the implied greater strength of hydrogen bonding in pure ethanol tetramers from the shorter O-O bond distance, which is also supported by the lower energy of pure ethanol tetramers as shown in Figure 2. In comparing these O-O bond distances with previous work on clusters with net cooperativity of 2, the conclu-

sion of tighter binding in these tetramers is supported; for example, in pure water decamers with cooperativity=2, the average O-O distance is between 2.74 and 2.80[35], and in pure water tetramers, this average O-O distance ranges from 2.74[36] to 2.85 Angstroms[37] depending on the conformer.

With this result, future work investigating the diverse range of 3-dimensional structures in mixed alcohol-water clusters of increasing size may further elucidate the pattern seen here in the O-O distance of mixed ethanol-water tetramers, in which each monomer serves as both a hydrogen bond acceptor and donor.

Table 1 Calculated and experimental rotational Constants of $(CH_3CH_2OH)_4$ conformers identified in spectra.

	2tg+g- DFT	Fitted 2tg+g-
Dipole	0.54	
μ_A	0.44	
μ_B	-0.28	
μ_C	-0.15	
A (MHz)	550.2	550.83 (6)
B (MHz)	530.9	539.16 (22)
C (MHz)	464.6	464.68(13)
D_J (kHz)	0.53	12.30 (23)
D_{JK} (kHz)	-0.32	-39.44 (5)
D_K (kHz)	0.11	27.74 (22)
d_1 (kHz)	.09	9.69 (8)
d_2 (kHz)	-0.15	-26.68 (16)
Error (kHz)		87
N		14

Table 2 Calculated and experimental rotational Constants of $H_2O(CH_3CH_2OH)_3$ conformers identified in spectra.

	wttt DFT	Fitted wttt	wg1g2t DFT	Fitted wg1g2t
Dipole	0.34		0.39	
μ_A	-0.25		-0.39	
μ_B	0.22		-0.05	
μ_C	-0.07		-0.05	
A (MHz)	981.9	982.11 (3)	1038.9	1036.86 (16)
B (MHz)	530.0	528.58 (17)	538.6	538.36 (5)
C (MHz)	355.1	355.20 (10)	382.4	381.67 (17)
D_J (kHz)	0.46	5.74 (5)	0.22	2.14 (8)
D_{JK} (kHz)	-0.84	-28.60 (5)	-0.30	-190.4 (4)
D_K (kHz)	0.42	23.70 (4)	1.26	188.3 (3)
d_1 (kHz)	0.15	1.34 (17)	0.67	24.52 (24)
d_2 (kHz)	-0.17	12.63 (30)	1.78	98.23 (16)
Error (kHz)		33		25
N		13		10

=

=

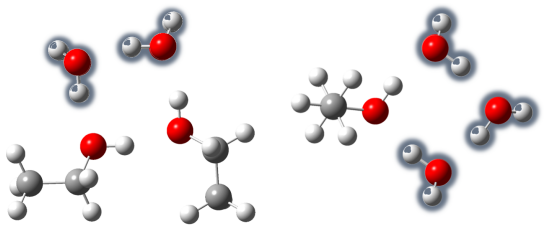

Fig. 4 Comparison of isotopically labeled clusters and actual hydrogen bond position for the wttw conformer of $(D_2O)_2(CH_3CH_2OH)_2$ and the gwww conformer of $(D_2O)_3(CH_3CH_2OH)$.

=

Table 3 Calculated and experimental rotational Constants of $(H_2O)_2(CH_3CH_2OH)_2$ conformers identified in spectra.

	wg1tw DFT	Fitted wg1tw	wttw DFT	Fitted wttw
Dipole	0.48		0.52	
μ_A	-0.47		-0.48	
μ_B	-0.09		-0.17	
μ_C	-0.05		0.14	
A (MHz)	1460.0	1458.78 (4)	1305.3	1305.26 (6)
B (MHz)	830.5	832.49 (24)	897.7	897.68 (8)
C (MHz)	586.7	587.02 (17)	552.9	552.91 (24)
D_J (kHz)	0.70	30.30 (21)	1.06	–
D_{JK} (kHz)	1.16	-88.40 (70)	-2.06	–
D_K (kHz)	-0.30	57.00 (5)	1.11	–
d_1 (kHz)	0.17	6.17 (12)	0.070	–
d_2 (kHz)	1.35	9.90 (13)	-0.44	–
Error (kHz)		74		96
N		12		10

Table 4 Calculated and experimental rotational Constants of $(H_2O)_3(CH_3CH_2OH)$ conformers identified in spectra.

	twww DFT	Fitted twww	gwww DFT	Fitted gwww
Dipole	0.29		0.39	
μ_A	-0.23		-0.28	
μ_B	-0.16		0.26	
μ_C	0.03		-0.07	
A (MHz)	3094.8	3093.50 (4)	2780.2	2780.97 (15)
B (MHz)	1189.9	1190.43 (26)	1257.2	1259.23 (26))
C (MHz)	903.3	903.33 (17)	990.8	990.44 (6)
D_J (kHz)	0.79	-49.57 (25)	2.50	–
D_{JK} (kHz)	-3.11	122.8 (10)	-9.31	–
D_K (kHz)	12.19	-72.0 (7)	20.35	–
d_1 (kHz)	0.18	33.91 (11)	0.20	–
d_2 (kHz)	1.14	-57.4 (3)	-1.03	–
Error (kHz)		44		79
N		9		5

=

4 Conclusions

This work has shown that tetramers of pure ethanol and mixed ethanol and water are formed in an array of low-energy conformers, with structural variation arising from the accessible gauche conformation states of ethanol sub-units. In the process of identifying tetramer structures with microwave signals, many potential minima were identified on the potential energy surfaces of these structures, demonstrating the myriad potential bonding patterns for these tetramers.

In particular, we see in this work that tetramer conformers that would otherwise be completely symmetric, i.e., one with all trans ethanol sub-units, are made polar by mixing ethanol and water in tetramer formation. These mixed clusters then both provide insight into mixing behavior of ethanol and water as well as rendering symmetric tetramer conformers polar, thus accessible experimentally.

It was interesting to note that although many different structures were computated as local energy minima for both the pure ethanol tetramers and mixed ethanol–water tetramers, only a few had sufficient dipole moments to be accessible experimentally. This highlights the importance of comparing experimental and computational studies of hydrogen bonding in small molecule clusters, as the full suite of low-energy conformations predicted by theoretical survey may not be observable. Experimental de-

tection of at least a few of the conformational variations possible enriches our understanding of the intermolecular dynamics of alcohol and water mixing at the few molecule scale, as computational surveys allow us to examine potential minima that we are blind to using rotational spectroscopy.

Further, this work assists in building towards a robust description of intermolecular dynamics and mixing of water and ethanol. In particular, the $(H_2O)_2(CH_3CH_2OH)_2$ structures identified in experimental spectra indicate that some tetramer structures formed by water and ethanol already show signs of micro-aggregation, with two water molecules on one side of the ring of hydrogen bonding, and two ethanol molecules on the other side. This is by no means the only available bonding pattern, as it has been shown that all of the available cyclical conformers of the $(H_2O)_2(CH_3CH_2OH)_2$ tetramer are close in energy, but it still indicates that this type of separation on the molecular scale is feasible for water and ethanol mixing. This observation may then assist in modeling the complex details of water and ethanol micro-aggregation that influence the dynamics of the bulk system, furthering understanding of this mixing and refining predictive models.

Author Contributions

We strongly encourage authors to include author contributions and recommend using CRediT for standardised contribution descriptions. Please refer to our general author guidelines for more information about authorship.

Conflicts of interest

There are no conflicts of interest to declare.

Acknowledgements

The authors gratefully acknowledge support from the NSF CSDM-A program (Grant CHE-1665467) and the NASA Laboratory Astrophysics program (Grant NNX-16AC75G). SED is supported by the National Science Foundation Graduate Research Fellowship Program (Grant DGE-1745301). Any opinions, findings, and conclusions or recommendations expressed in this material are those of the authors and do not necessarily reflect the views of the National Science Foundation.

Notes and references

1 F. N. Keutsch and R. J. Saykally, *Proceedings of the National Academy of Sciences*, 2001, **98**, 10533–10540.

2 W. B. Bosma, L. E. Fried and S. Mukamel, *The Journal of Chemical Physics*, 1993, **98**, 4413–4421.

3 R. S. Fellers, *Science*, 1999, **284**, 945–948.

4 B. J. Smith, D. J. Swanton, J. A. Pople, H. F. Schaefer and L. Radom, *The Journal of Chemical Physics*, 1990, **92**, 1240–1247.

5 W. T. S. Cole, R. S. Fellers, M. R. Viant, C. Leforestier and R. J. Saykally, *The Journal of Chemical Physics*, 2015, **143**, 154306.

6 M. Jarrahi, *IEEE Transactions on Terahertz Science and Technology*, 2015, **5**, 391–397.

7 N. T. Yardimci, S. Cakmakyapan, S. Hemmati and M. Jarrahi, *Scientific Reports*, 2017, **7**,.

8 I. Juurinen, K. Nakahara, N. Ando, T. Nishiumi, H. Seta, N. Yoshida, T. Morinaga, M. Itou, T. Ninomiya, Y. Sakurai, E. Salonen, K. Nordlund, K. Hämäläinen and M. Hakala, *Phys. Rev. Lett.*, 2011, **107**, 197401.

9 A. K. Soper, L. Dougan, J. Crain and J. L. Finney, *The Journal of Physical Chemistry B*, 2005, **110**, 3472–3476.

10 C. Calabrese, B. Temelso, I. Usabiaga, N. A. Seifert, F. J. Basterretxea, G. Prampolini, G. C. Shields, B. H. Pate, L. Evangelisti and E. J. Cocinero, *Angewandte Chemie International Edition*, 2021.

11 E. M. Neeman and T. R. Huet, *Physical Chemistry Chemical Physics*, 2021, **23**, 2179–2185.

12 S. Lenton, N. H. Rhys, J. J. Towey, A. K. Soper and L. Dougan, *The Journal of Physical Chemistry B*, 2018, **122**, 7884–7894.

13 N. N. Nyamweya and K. O. Abuga, 2021.

14 K. Abuga and N. Nyamweya, *Pharmacy*, 2021, **9**, 64.

15 G. G. Brown, B. C. Dian, K. O. Douglass, S. M. Geyer, S. T. Shipman and B. H. Pate, *Review of Scientific Instruments*, 2008, **79**, 053103.

16 G. J. Mead, E. R. Alonso, I. A. Finneran, P. B. Carroll and G. A. Blake, *Journal of Molecular Spectroscopy*, 2017, **335**, 68–73.

17 M. Juanes, W. Li, L. Spada, L. Evangelisti, A. Lesarri and W. Caminati, *Physical Chemistry Chemical Physics*, 2019, **21**, 3676–3682.

18 D. Loru, I. Peña and M. E. Sanz, *Physical Chemistry Chemical Physics*, 2019, **21**, 2938–2945.

19 S. Khemissi, A. P. Salvador and H. V. L. Nguyen, *The Journal of Physical Chemistry A*, 2021, **125**, 8542–8548.

20 L. Ferres, J. Cheung, W. Stahl and H. V. L. Nguyen, *The Journal of Physical Chemistry A*, 2019, **123**, 3497–3503.

21 S. M. Mejía, J. F. Espinal and F. Mondragón, *Journal of Molecular Structure: THEOCHEM*, 2009, **901**, 186–193.

22 M. J. Frisch, G. W. Trucks, H. B. Schlegel, G. E. Scuseria, M. A. Robb, J. R. Cheeseman, G. Scalmani, V. Barone, B. Mennucci, G. A. Petersson, H. Nakatsuji, M. Caricato, X. Li, H. P. Hratchian, A. F. Izmaylov, J. Bloino, G. Zheng, J. L. Sonnenberg, M. Hada, M. Ehara, K. Toyota, R. Fukuda, J. Hasegawa, M. Ishida, T. Nakajima, Y. Honda, O. Kitao, H. Nakai, T. Vreven, J. A. Montgomery, Jr., J. E. Peralta, F. Ogliaro, M. Bearpark, J. J. Heyd, E. Brothers, K. N. Kudin, V. N. Staroverov, R. Kobayashi, J. Normand, K. Raghavachari, A. Rendell, J. C. Burant, S. S. Iyengar, J. Tomasi, M. Cossi, N. Rega, J. M. Millam, M. Klene, J. E. Knox, J. B. Cross, V. Bakken, C. Adamo, J. Jaramillo, R. Gomperts, R. E. Stratmann, O. Yazyev, A. J. Austin, R. Cammi, C. Pomelli, J. W. Ochterski, R. L. Martin, K. Morokuma, V. G. Zakrzewski, G. A. Voth, P. Salvador, J. J. Dannenberg, S. Dapprich, A. D. Daniels, Ő. Farkas, J. B. Foresman, J. V. Ortiz, J. Cioslowski and D. J. Fox, *Gaussian09 Revision E.01*, Gaussian Inc. Wallingford CT 2009.

23 I. A. Finneran, D. B. Holland, P. B. Carroll and G. A. Blake, *Review of Scientific Instruments*, 2013, **84**, 083104.

24 S. E. Dutton and G. A. Blake, *Physical Chemistry Chemical Physics*, 2022, **24**, 13831–13838.

25 D. Loru, I. Peña and M. Sanz, *Journal of Molecular Spectroscopy*, 2017, **335**, 93–101.

26 H. PICKETT, R. POYNTER, E. COHEN, M. DELITSKY, J. PEARSON and H. MÜLLER, *Journal of Quantitative Spectroscopy and Radiative Transfer*, 1998, **60**, 883–890.

27 Z. Kisiel, *Spectroscopy from Space*, Springer Netherlands, 2001, pp. 91–106.

28 J. Durig and R. Larsen, *Journal of Molecular Structure*, 1990, **238**, 195–222.

29 H. Hartwig and H. Dreizler, *Zeitschrift für Naturforschung A*, 1996, **51**, 923–932.

30 J. Pal, A. Patla and R. Subramanian, *Chemosphere*, 2021, **272**, 129846.

31 W. Sun and M. Schnell, *Angewandte Chemie International Edition*, 2022, **61**,.

32 C. Pérez, S. Lobsiger, N. A. Seifert, D. P. Zaleski, B. Temelso, G. C. Shields, Z. Kisiel and B. H. Pate, *Chemical Physics Letters*, 2013, **571**, 1–15.

33 S. Maeda and K. Ohno, *The Journal of Physical Chemistry A*, 2007, **111**, 4527–4534.

34 C. Pérez, M. T. Muckle, D. P. Zaleski, N. A. Seifert, B. Temelso, G. C. Shields, Z. Kisiel and B. H. Pate, *Science*, 2012, **336**, 897–901.

35 C. Pérez, D. P. Zaleski, N. A. Seifert, B. Temelso, G. C. Shields, Z. Kisiel and B. H. Pate, *Angewandte Chemie International Edition*, 2014, **53**, 14368–14372.

36 J. F. Pérez, C. Z. Hadad and A. Restrepo, *International Journal of Quantum Chemistry*, 2008, **108**, 1653–1659.

37 R. Ludwig, *Angewandte Chemie International Edition*, 2001, **40**, 1808–1827.